DEC 23 1946

ARR No. L5F25b

[redacted]

NATIONAL ADVISORY COMMITTEE FOR AERONAUTICS

WARTIME REPORT

ORIGINALLY ISSUED
September 1945 as
Advance Restricted Report L5F25b

STATIC-THRUST TESTS OF SIX ROTOR-BLADE DESIGNS ON A HELICOPTER IN THE LANGLEY FULL-SCALE TUNNEL

By Richard C. Dingeldein and Raymond F. Schaefer

Langley Memorial Aeronautical Laboratory
Langley Field, Va.

NACA

WASHINGTON

NACA ARR No. L5F25b [redacted]

NATIONAL ADVISORY COMMITTEE FOR AERONAUTICS

ADVANCE RESTRICTED REPORT

STATIC-THRUST TESTS OF SIX ROTOR-BLADE DESIGNS ON A HELICOPTER IN THE LANGLEY FULL-SCALE TUNNEL

By Richard C. Dingeldein and Raymond F. Schaefer

SUMMARY

Measurements of the static-thrust performance of six sets of rotor blades mounted on a helicopter fuselage have been made in the Langley full-scale tunnel. The rotor blades differ in surface condition, pitch distribution, airfoil section, plan form, and solidity. These differences are largely unsystematic. The variation of rotor thrust coefficient with torque coefficient and the power required to hover are compared for each set of blades. Because of the indeterminate condition of ground restraint caused by the wind-tunnel balance house and test-chamber walls, the absolute magnitude of the data is questionable but the comparative results are believed to be reliable.

A rotor of conventional construction having a doped fabric surface and relatively wide rib spacing required the most power to hover. The best hovering performance was given by two sets of plywood-covered blades of relatively low solidity, which required only slightly less power than a smoother and more rigidly constructed version of the conventional blades. The results indicate that the rotor-blade surface condition has a very important effect upon performance and that the optimum performance of any rotor design will be obtained only if the blades have a smooth and accurately contoured surface that will not deform during flight. The results further indicate that significant reductions in power can be obtained for this aircraft by the use of lower rotor speeds.

INTRODUCTION

Tests to determine the performance characteristics of a helicopter over a range of airspeeds were conducted in the Langley full-scale tunnel. This report presents measurements of the static-thrust performance of six sets of rotor blades supplied by the Air Technical Service Command, Wright Field. These sets of blades differ in

[redacted]

surface condition, pitch distribution, airfoil section, plan form, and solidity. The differences are largely unsystematic. The results of these tests are presented and the performance of the rotor blades in typical hovering conditions is compared. In addition, measurements of the rotor-blade surface roughness are included and the effect of surface condition on performance is discussed.

SYMBOLS

C_T thrust coefficient of main rotor $\left(\frac{T}{\rho(\Omega R)^2 \pi R^2}\right)$

C_Q torque coefficient of main rotor $\left(\frac{Q}{\rho(\Omega R)^2 \pi R^3}\right)$

T rotor thrust, pounds

Q rotor torque, foot-pounds

Ω angular velocity of rotor, radians per second

ρ mass density of air, slugs per cubic foot

R rotor-blade radius, feet

σ rotor solidity $\left(\frac{bc_e}{\pi R}\right)$

b number of rotor blades

c_e equivalent chord $\left(\frac{\int_0^R cr^2\,dr}{\int_0^R r^2\,dr}\right)$

r distance from center of rotation to blade element

c rotor-blade chord at radius r

APPARATUS

The helicopter was mounted at the three landing-gear supports on a six-component strain-gage balance. A photograph of the test setup is shown as figure 1. The center-of-gravity location for the tests was chosen as the point on the center line of the rotor shaft 56.52 inches below the plane of the flapping hinges. This location was based on information supplied by the manufacturer and falls within the center-of-gravity range that corresponds to normal gross weight.

A strain-gage-type torque meter mounted on the main rotor shaft measured the torque input to the rotor. The total-pitch angle was measured by an indicator attached to the control linkage and was calibrated against a protractor mounted on a rotor blade at the 14.25-foot radius. The indicators for the blade pitch angle, strain-gage balance, and torque meter, together with the remote-control system that operated the engine and flight controls of the helicopter, were located in a test house at the rear of the balance house. (See fig. 1.)

Observations of the surface roughness of the six sets of rotor blades were made with a 40-power microscope. A prism attachment permitted measurement of the height of the roughness particles.

ROTOR BLADES

The geometric characteristics of each of the rotor blades are presented in table I and figure 2, and photographs of the blades are shown as figure 3.

Description of Rotor Blades

The blades of rotor A, which are the production blades of the helicopter tested, have a radius of 19 feet measured from the center of rotation. The blades are tapered in plan form, have a total area (three blades) of 65.4 square feet, are untwisted, and have an NACA 0012 airfoil section. Each blade consists of a tubular steel spar to which 36 wooden ribs are attached. The rib spacing is approximately 6 inches at the blade root and decreases to $4\frac{1}{2}$ inches at the tip. The forward portion, which comprises approximately 35 percent of the chord, is contoured by spruce fairing strips. A wire cable forms the trailing edge and the entire rotor blade is fabric-covered.

The forward portion of the blades of rotor B has been accurately built up to contour for 35 percent of the chord from the 40-percent radius outboard to the tip. This surface is very smooth and the entire rotor blade was polished with wax prior to each test. The blades have the same rib spacing as the blades of rotor A from the root to the eleventh rib (44-percent radius) but have intermediate ribs inserted from this station to the tip, which make a total of 61 ribs for these blades as compared with 36 ribs for the blades of rotor A. With the exceptions of the smooth leading edge and the rib spacing, the blades of rotor B are identical to those of rotor A.

The blades of rotor C have a linear washout of 0.42° per foot and the same rib spacing as that used in rotor B. The blade dimensions, airfoil section, surface finish, forward-portion contour, and method of construction are the same as for rotor A.

The blades of rotor D have a radius of 18 feet, which is 1 foot less than the radius of the other blades tested. The plan form is rectangular and the three blades have a total area of 52.6 square feet. These blades have a linear washout of 0.66° per foot and an NACA 0012 airfoil section. Each blade has 58 ribs with a 4-inch spacing at the blade root, which gradually decreases to 2 inches at the tip. The forward portion is contoured similarly to the blades of rotor B. The type of construction is the same as that of rotors A, B, and C.

The blades of rotor E have a radius of 19 feet, a tapered plan form, and a total area of 46.3 square feet. The airfoil section is an NACA 23015 section with the rearward 10 percent of the mean line reflexed 0.9°. The blades are covered with plywood and have a 7-percent-chord brass leading-edge abrasion strip that extends along the outboard 44 percent of the span. There is a balancing tab located near the blade tip. (See fig. 2.)

The blades of rotor F have a linear washout of 0.45° per foot but are otherwise the same as the blades of rotor E.

Rotor-Blade Surface Roughness

After the static-thrust tests had been completed, the surface roughness of each rotor was determined. The amplitude and frequency of the rotor-blade surface waves were measured at the 80-percent radius on the upper and lower surfaces approximately $1\frac{1}{2}$ inches from the leading and the trailing edges of each rotor blade. The surface roughness of rotors A, B, C, and D is primarily due to the fabric weave. The pigmented-dope finish partly filled the small depressions and left a wavy surface. The amplitude of the waves is approximately 0.0011 inch and the spanwise and chordwise frequency on both the upper and lower blade surfaces ranges from 79 to 106 waves per inch. The contoured forward portion on the blades of rotors B and D is aerodynamically smooth. It was not possible to measure the surface roughness of rotors E and F with the microscope used, although these two rotors have definite contour defects. Between the leading-edge strip and the plywood covering on both rotors E and F there was a U-shaped furrow approximately 1/64 to 1/32 inch wide and deep. The furrows in the blades of rotor E were filled for all the tests, but those in the blades of rotor F were filled for the second series of measurements only. In spite of the application of filler to the most pronounced discontinuities, the blade contour differs noticeably from the true airfoil section because of flat spots and protuberances, the elimination of which would require a complete resurfacing of the blades.

TEST PROCEDURE

The static-thrust tests were made at a rotor-shaft tilt of 0° and with the longitudinal and lateral feathering controls locked in the neutral position. Data are presented for engine speeds ranging from 1600 to 2100 rpm (rotor speeds of 171 to 225 rpm) for indicated total-pitch angles from 4° to 12°. The helicopter was trimmed for zero yawing moment about the center of gravity throughout the tests by adjusting the pitch angle of the tail rotor. Static-thrust measurements were first taken for four sets of rotor blades and the tests were later repeated for all six rotors. The two rotors for which only one test was made are rotors C and E.

RESULTS AND DISCUSSION

Thrust and Torque Coefficients

The results of the two static-thrust tests are presented in figure 4 for each set of rotor blades in terms of the thrust and torque coefficients of the rotor and the indicated total-pitch angles. The coefficients shown for rotor D are referred to the same disk area as those for the other rotors, instead of to the actual 36-foot-diameter disk, in order to compare the blades on the basis of thrust available for the helicopter tested. These coefficients, however, were also calculated for the 36-foot-diameter disk and the faired curve was found to be almost coincident with the curve of figure 4(d) for thrust coefficients between 0.0030 and the maximum covered in the tests.

The data are consistent for rotors C, D, E, and F, but there is considerable scatter in the results for rotors A and B. This scatter probably results from zero drifting in the lift strain-gage-indicator readings, which occurred throughout the tests but was most pronounced during tests of these two rotors. The thrust data have been corrected for zero drifting by assuming that the drifting varied linearly with time.

The second series of data obtained for rotor A and rotor B (figs. 4(a) and 4(b)) shows a variation with rotor speed. Inasmuch as this variation is not apparent for the first series of data obtained for these blades and does not occur for any of the other rotors in either series of tests, only one curve is faired through the test points.

A comparison of the static-thrust performance of all the rotor blades based on the conventional production rotor radius of 19 feet is shown in figure 5. It is emphasized that the absolute magnitude of the data presented is questionable because of the unusual ground effect of the balance-house roof (see fig. 1) and possible restraint of the test-chamber walls on the air-flow pattern, but the comparative results are believed to be reliable.

Power Required for Hovering

The main-rotor shaft power required for the helicopter to hover at sea level with each set of rotor blades has been estimated from figure 5 and is given in table II. The calculations are presented for rotor-thrust coefficients of 0.00387 and 0.00464, which correspond to a gross weight of 2500 pounds, a rotor-shaft tilt of 0°, and engine speeds of 2300 and 2100 rpm (rotor speeds of 246 and 225 rpm), respectively. The percentage less horsepower required for each set of blades, referred to rotor A, is also included.

The results indicate that rotor A requires approximately 148 and 140 horsepower for hovering at engine speeds of 2300 and 2100 rpm, respectively. The curves of figure 5 also predict that rotor C will permit the helicopter to hover with an average of 7 percent less power than rotor A and that more then 3 percent additional power would be saved if rotor B were installed. Rotor D would require an average of 4 percent less power than rotor A. Rotors E and F would need approximately 12 and 13 percent less power, respectively, to hover than rotor A.

The thrust in excess of 2500 pounds that the five experimental rotors would produce at engine speeds of 2300 and 2100 rpm for the same power input that the production blades (rotor A) require to hover (approximately 148 and 140 horsepower, respectively) is also included in table II. The greatest single gain is shown at 2300 rpm by the blades of rotor F; for a power input of approximately 148 horsepower, these blades produce almost 300 pounds more thrust than the blades of rotor A.

The advantage of operating rotors at lower rotational speeds and thus effecting a reduction in profile drag is clearly shown by the data in table II. Almost 8 horsepower would be saved in hovering with rotor A by operating at an engine speed of 2100 rpm instead of 2300 rpm (rotor speeds of 225 and 246 rpm, respectively). The power required for hovering with each rotor continues to decrease with increasing thrust coefficient for values of C_T as high as 0.00582 (an engine speed of 1375 rpm or a rotor speed of 201 rpm). At this thrust coefficient, which is the highest afforded by the data, rotors A and F require approximately 136 and 119 horsepower, respectively. (See fig. 5.)

The relative performance of rotors E and F indicates that linear washout results in increased efficiency at the higher thrust coefficients. The magnitude of this effect cannot be accurately estimated from these data, however, because of the limits of experimental accuracy and the surface differences between these rotor blades.

Effect of Rotor-Blade Surface on Performance

The results of figure 5 indicate that for the blades tested and the conditions covered the surface roughness, the accuracy of the rotor-blade contour, and the rigidity of the rotor-blade surface are the most important factors affecting static-thrust performance. For a given thrust, rotor A required more power throughout the range of total-pitch angle than any of the other rotors tested. The other rotors, however, had either a smoother surface or a more accurately and permanently contoured surface, or both. The improvements in the performance of fabric-covered blades that result from having close rib spacing and a smooth and accurately contoured forward portion are clearly indicated by the performance of rotor B. The performance of rotor D is not so good as would be expected for a rotor having blades with an accurately contoured forward portion and very close rib spacing. An inspection of these blades, however, showed that the fabric is loosely attached to several ribs and on one blade it is not fastened at all to two ribs near the blade tip. The fabric bulge that resulted during operation is apparent in high-speed photographs of the rotor blade and is therefore believed to be responsible for a noticeable decrease in performance. Because of differences in solidity, blade thickness, camber, and type of surface imperfection, a comparison of the blades of rotors E and F with the other blades on the basis of surface condition cannot be made. Rotors E and F would be expected to have a better performance at any given thrust coefficient as a result of their lower solidity.

CONCLUSIONS

The following conclusions were drawn from static-thrust tests of six sets of rotor blades mounted on a helicopter fuselage in the Langley full-scale tunnel:

1. The condition of the rotor-blade surface has a large effect upon the rotor performance. The optimum performance of any rotor design will be obtained only if the blades have a smooth and accurately contoured surface that will not deform during flight.

2. The production rotor, rotor A, requires more power to produce a given thrust throughout the range of total-pitch angle than any of the other blades tested. It is estimated that 148 and 140 horsepower are needed for these blades to hover at thrust coefficients of 0.00387 and 0.00464, respectively, which correspond to a gross weight of 2500 pounds and engine speeds of 2300 and 2100 rpm. The average saving in power required to hover at these thrust coefficients by rotors B, C, D, E, and F is approximately 10, 7, 4, 12, and 13 percent, respectively. For the same power input that rotor A requires to hover at an engine speed of 2300 rpm, rotor F will produce nearly 300 pounds more thrust.

3. The reduction in power required to hover that may be obtained by operating at lower rotor speeds is clearly shown for the blades tested. Savings of as much as 8 horsepower are obtained by hovering at an engine speed of 2100 rpm as compared to 2300 rpm (thrust coefficients of main rotor C_T, 0.00464 and 0.00387, respectively). The data indicate additional savings with further reduction in engine speed to values at least as low as 1875 rpm (C_T = 0.00532), which is the lowest engine speed afforded by the data when a gross weight of 2500 pounds is assumed.

4. Linear washout appears to result in increased efficiency at the higher thrust coefficients, as indicated by the relative performance of rotors E and F. The magnitude of this effect cannot be accurately estimated from these data, however, because of the limits of experimental accuracy and the surface differences between these rotors.

Langley Memorial Aeronautical Laboratory
National Advisory Committee for Aeronautics
Langley Field, Va.

TABLE I.- GEOMETRIC CHARACTERISTICS OF ROTOR BLADES

Rotor	Rotor-blade radius (ft)	Airfoil section	Linear washout (deg/ft)	Root chord (in.)	Tip chord (in.)	Area of three blades (sq ft)	Rotor solidity, σ
A	19	NACA 0012	0	20	9.88	65.4	0.060
B	19	NACA 0012	0	20	9.88	65.4	.060
C	19	NACA 0012	0.42	20	9.88	65.4	.060
D	18	NACA 0012	.66	14.4	14.40	52.6	.061
E	19	Modified NACA 23015	0	12.5	6.75	46.3	.042
F	19	Modified NACA 23015	.45	12.5	6.75	46.3	.042

NATIONAL ADVISORY
COMMITTEE FOR AERONAUTICS

TABLE II.- ESTIMATE OF MAIN-ROTOR SHAFT POWER REQUIRED FOR HELICOPTER

TO HOVER AT SEA LEVEL WITH ROTORS TESTED

Rotor	Engine speed, rpm					
	2300			2100		
	$C_T = 0.00387$			$C_T = 0.00464$		
	Horsepower required to hover	Percent less power required than for rotor A	Excess thrust for 147.7 hp (1)	Horsepower required to hover	Percent less power required than for rotor A	Excess thrust for 140.0 hp (1)
A	147.7	------------	0	140.0	------------	0
B	131.1	11.2	233	126.9	9.4	182
C	137.4	7.0	155	130.8	6.6	128
D	140.8	4.7	97	134.8	3.7	74
E	127.6	13.6	278	124.7	10.9	215
F	128.2	13.2	278	123.4	11.9	258

[1]Thrust in excess of the assumed gross weight of 2500 lb which would be produced by each rotor for the same power input that rotor A requires to hover.

NATIONAL ADVISORY
COMMITTEE FOR AERONAUTICS

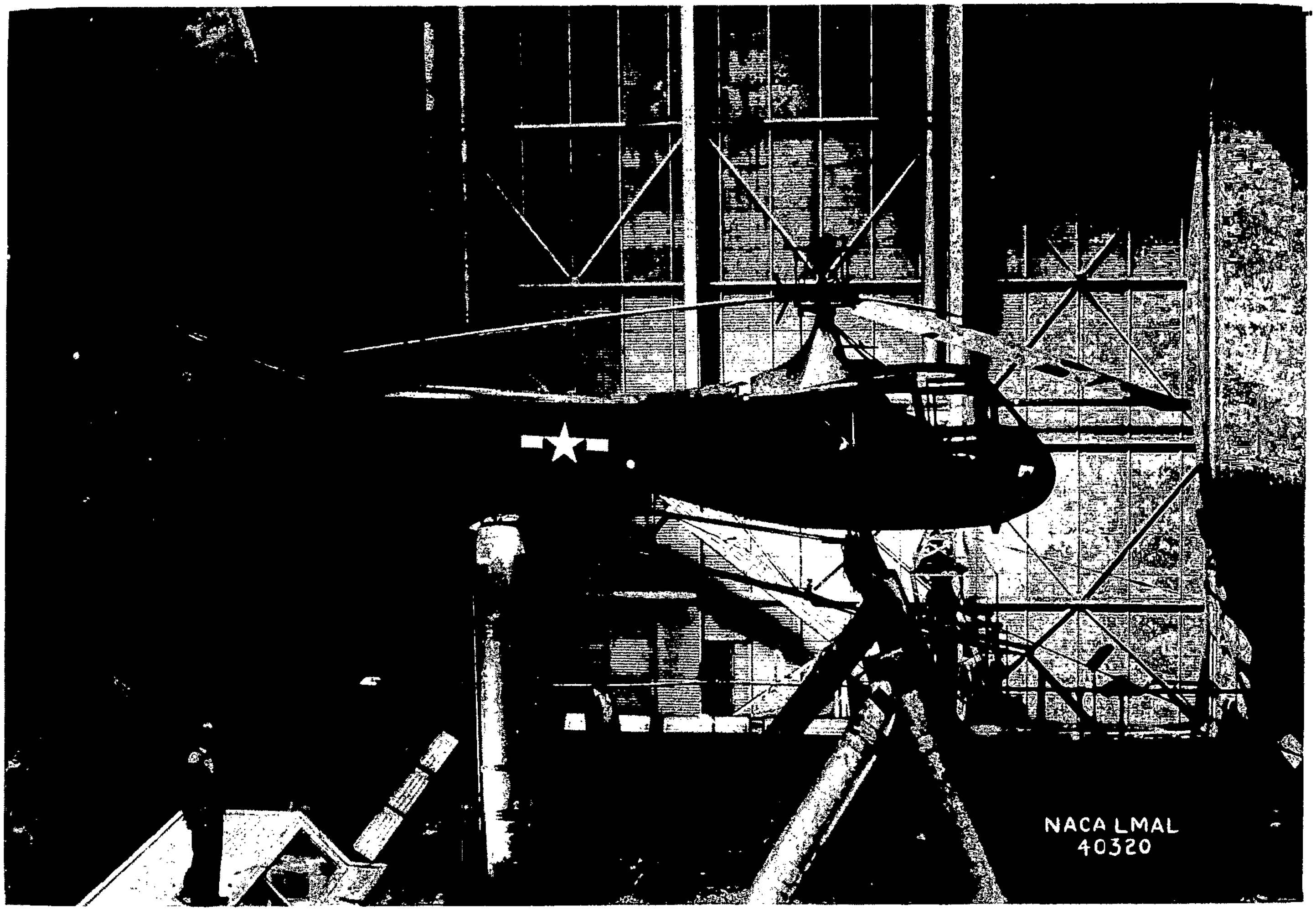

Figure 1.- Helicopter with production rotor (rotor A) mounted in Langley full-scale tunnel.

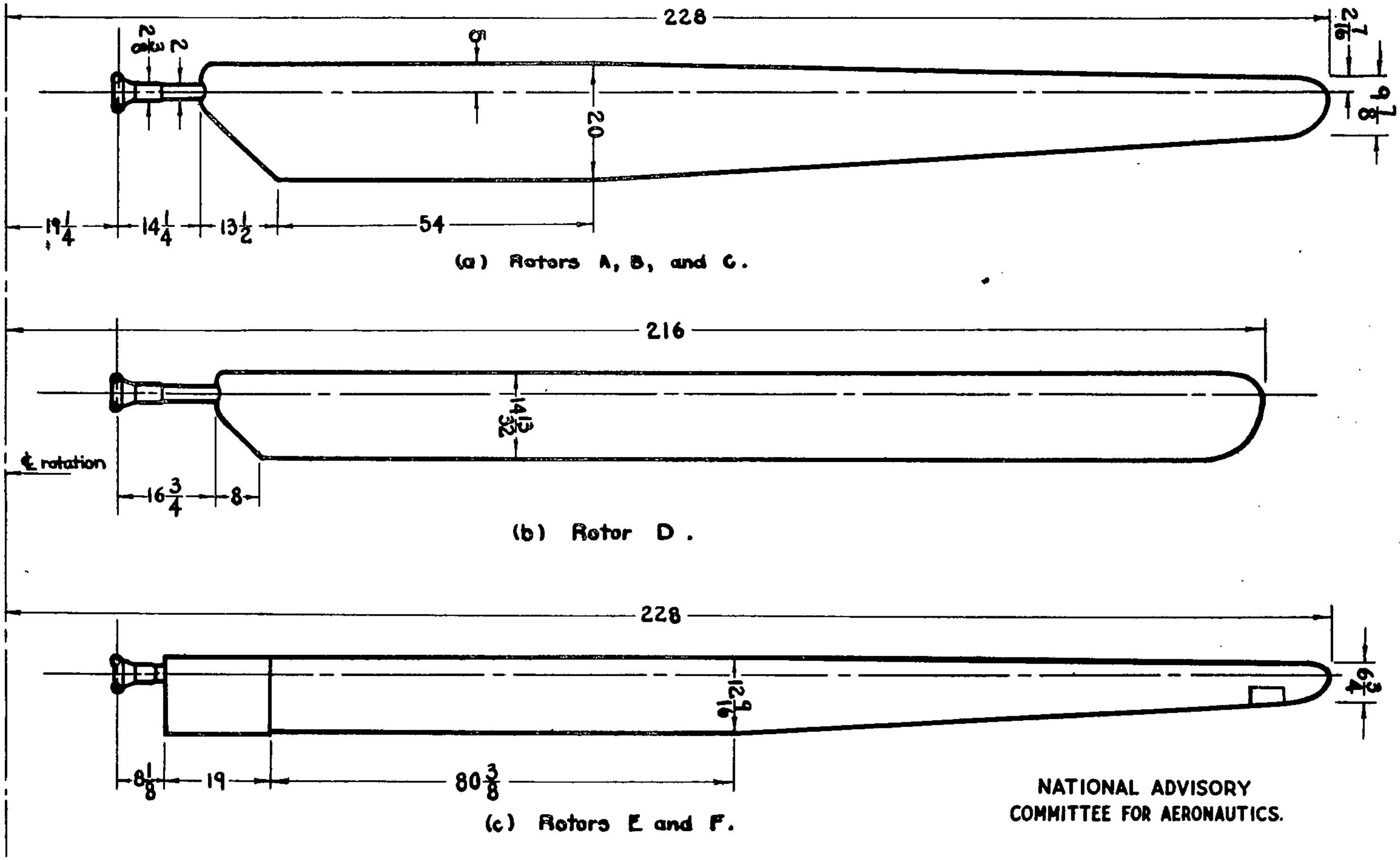

Figure 2. - Rotor blades tested in static thrust.
(All dimensions given in inches.)

(a) Rotor A.

(b) Rotor B.

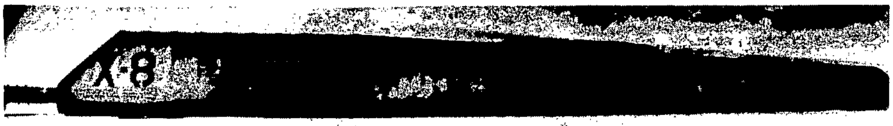

(c) Rotor C.

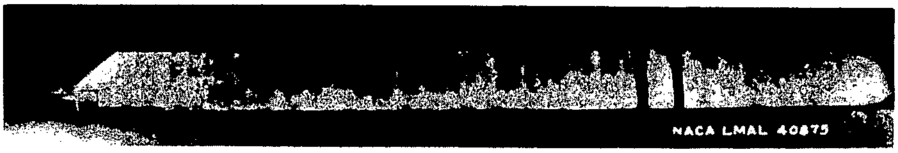

(d) Rotor D.

e) Rotor E.

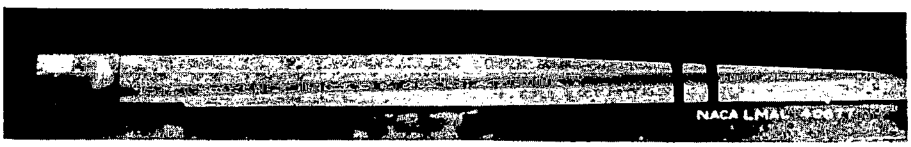

(f) Rotor F.

Figure 3.- Lower-surface views of a blade
from each rotor tested on helicopter
for static-thrust performance.

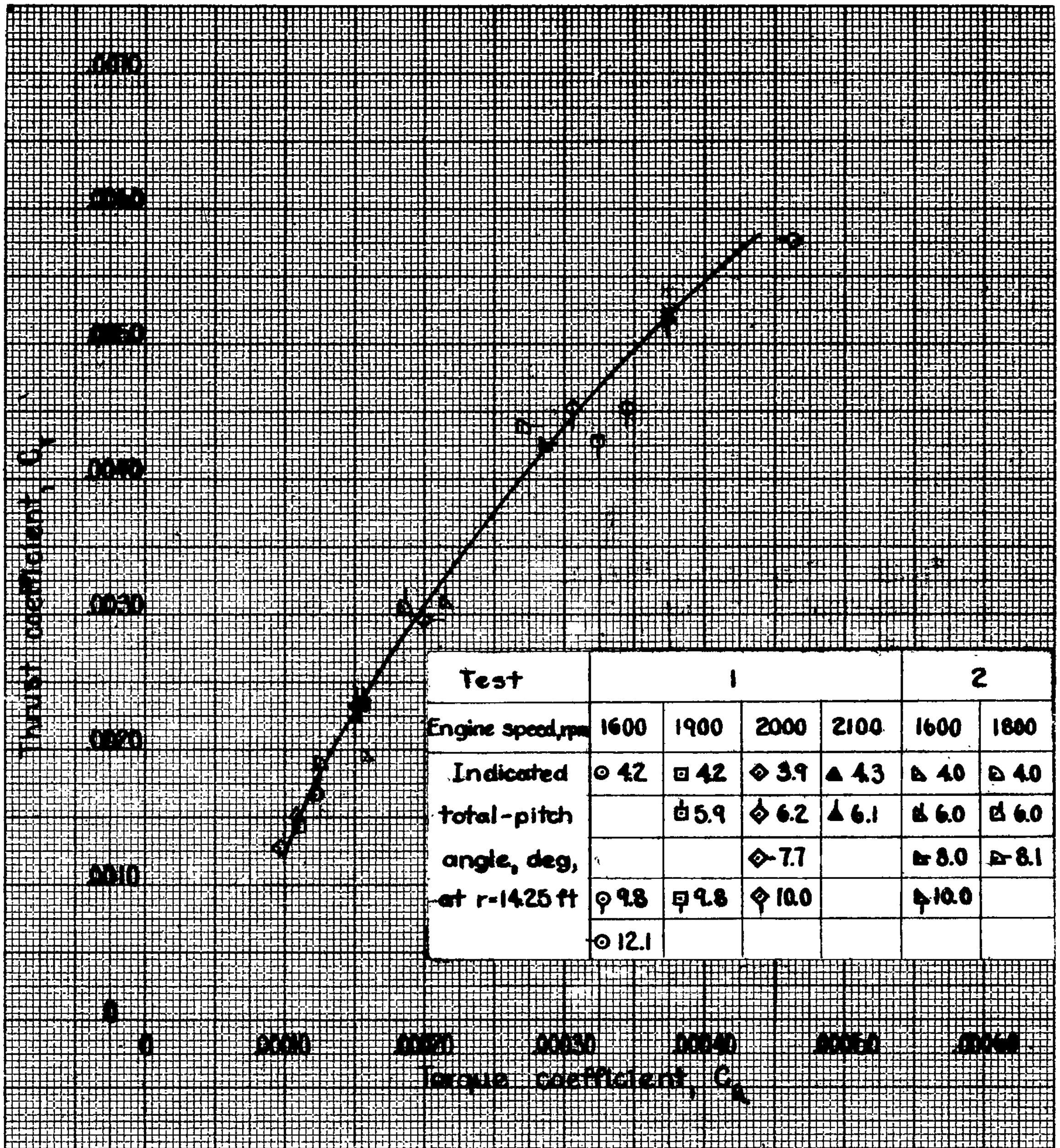

(a) Rotor A.

NATIONAL ADVISORY
COMMITTEE FOR AERONAUTICS

Figure 4. - Static-thrust performance of rotors tested.

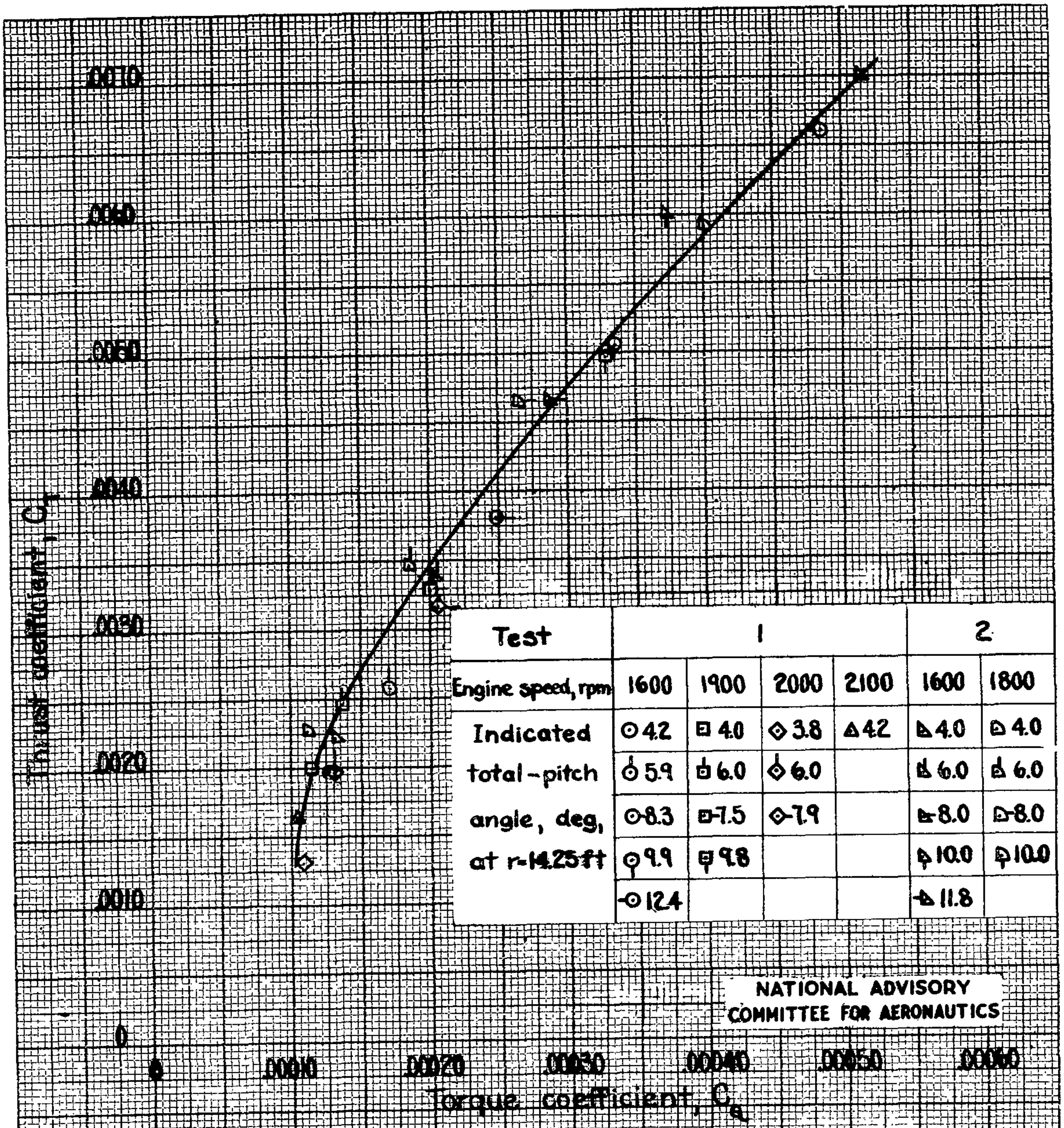

(b) Rotor B.

Figure 4.- Continued.

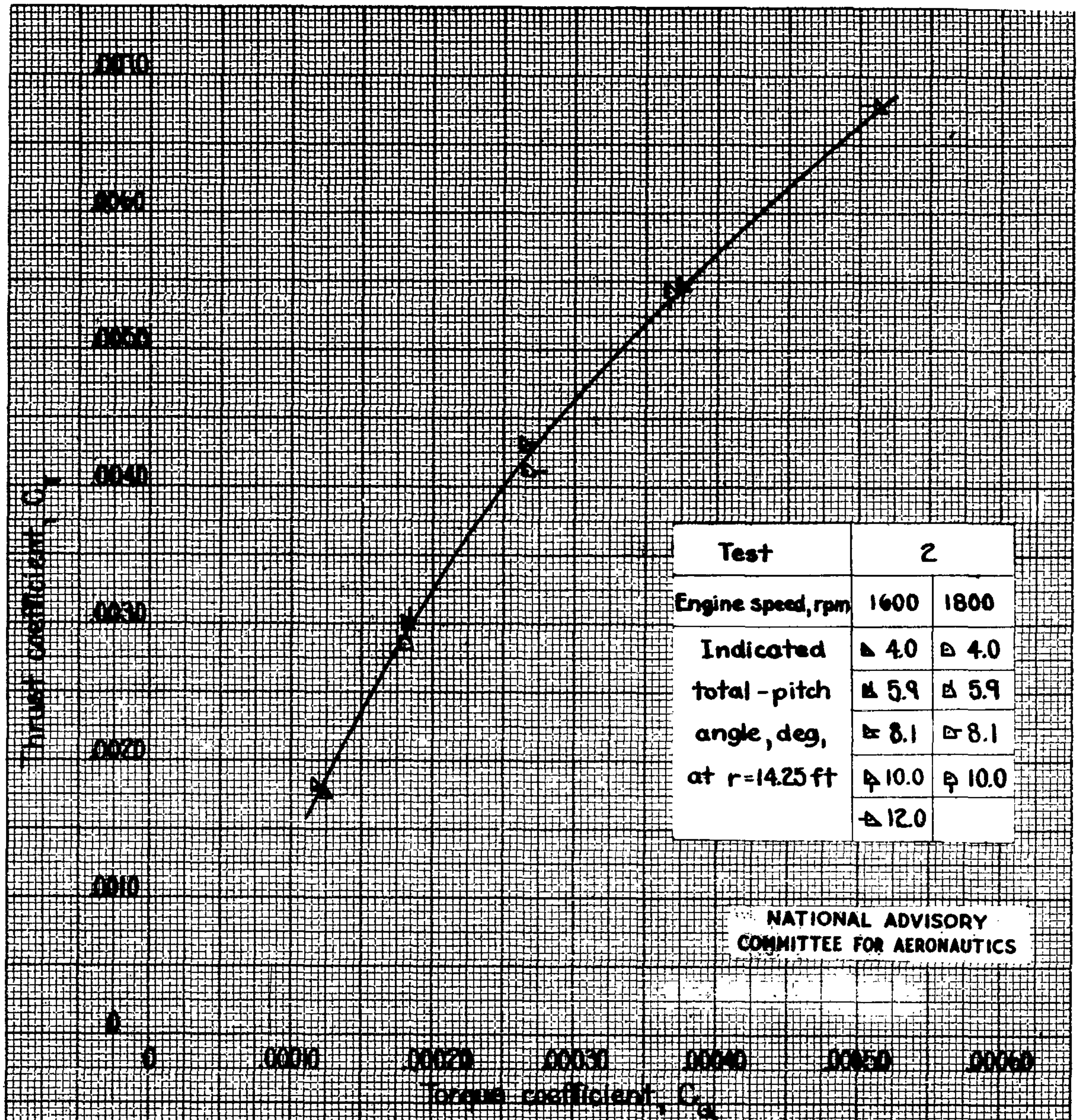

(c) Rotor C.

Figure 4.- Continued.

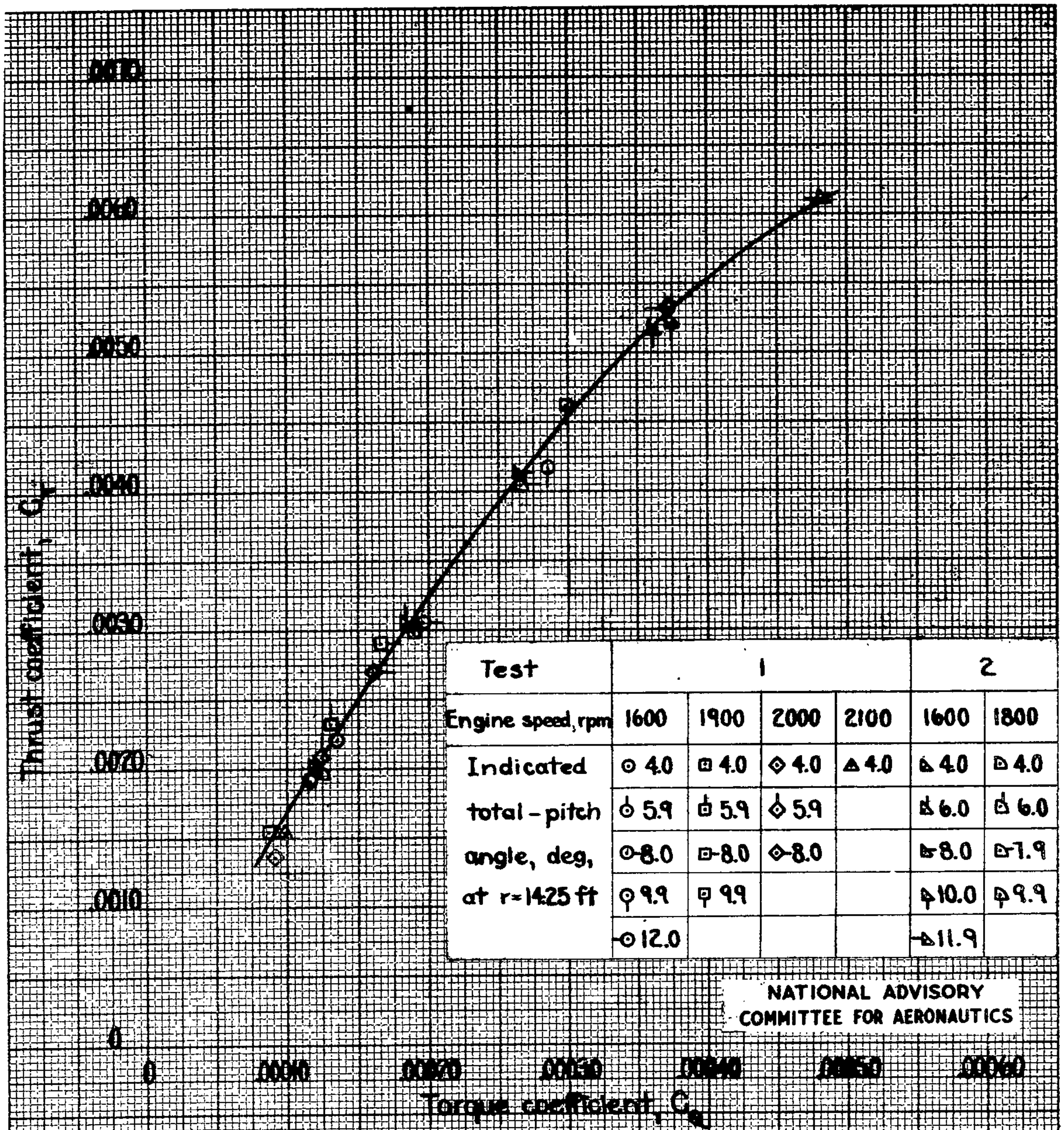

(d) Rotor D (coefficients based on 19-foot radius).

Figure 4.- Continued.

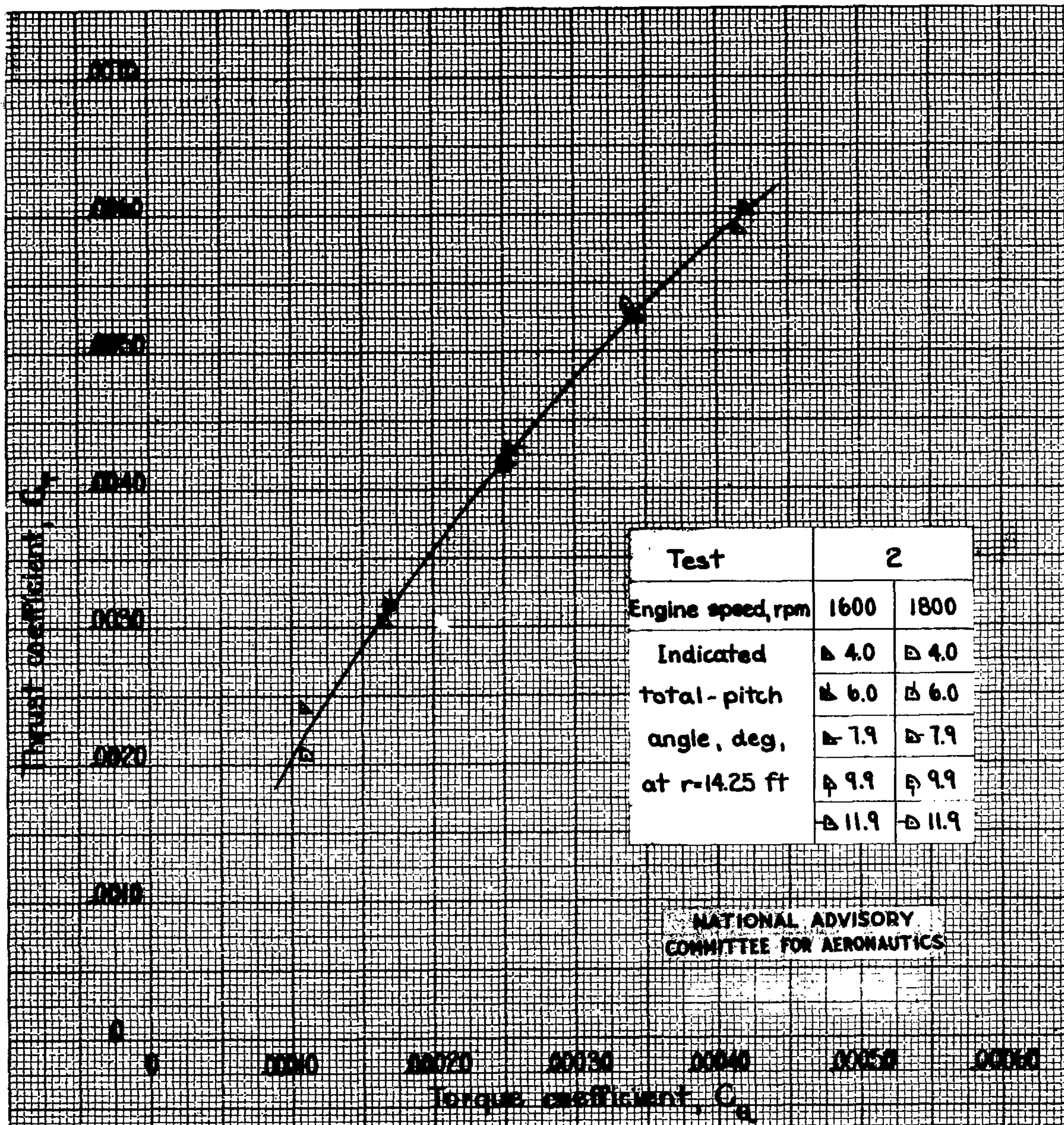

(e) Rotor E.

Figure 4.- Continued.

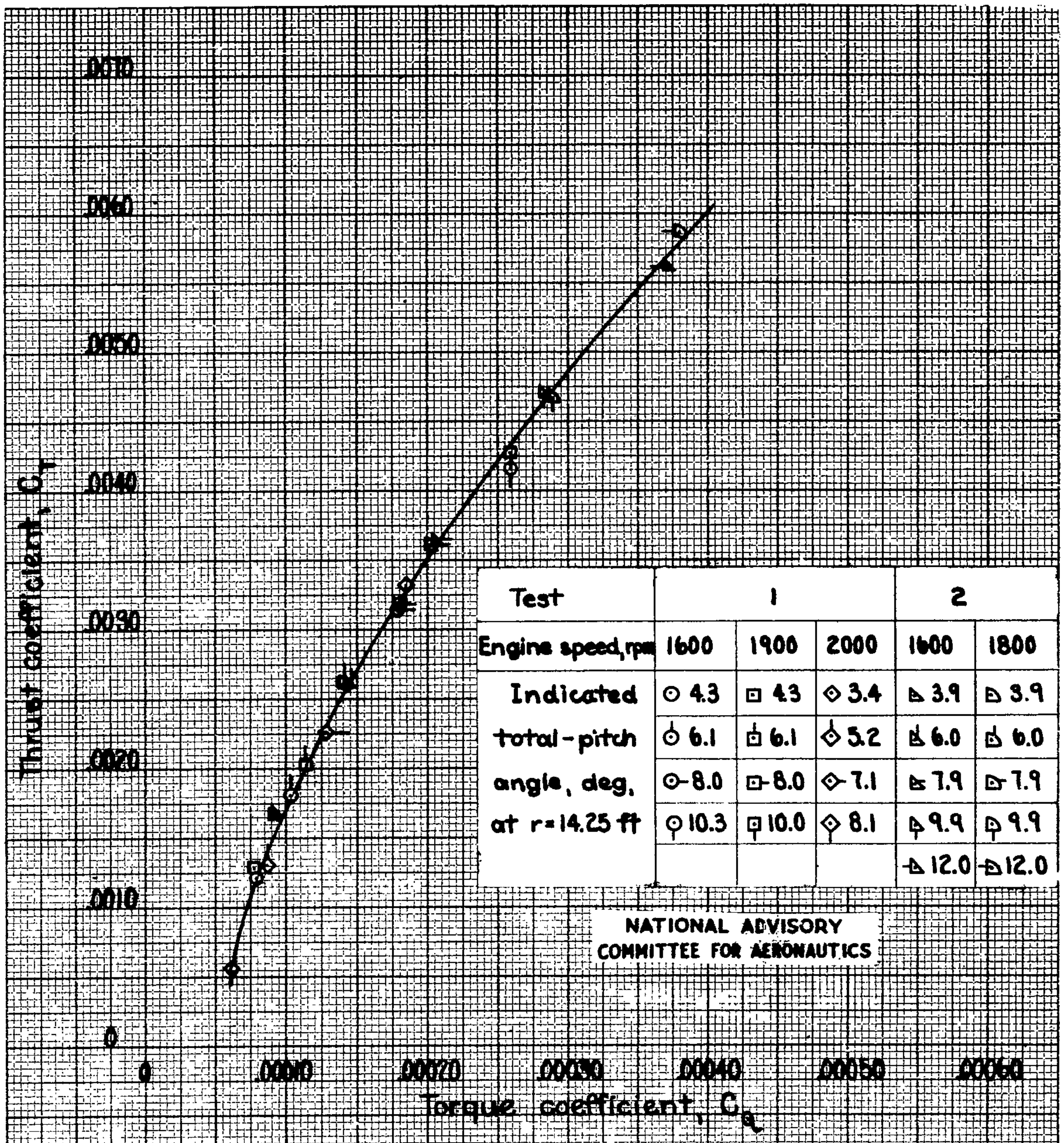

(f) Rotor F.

Figure 4.- Concluded.

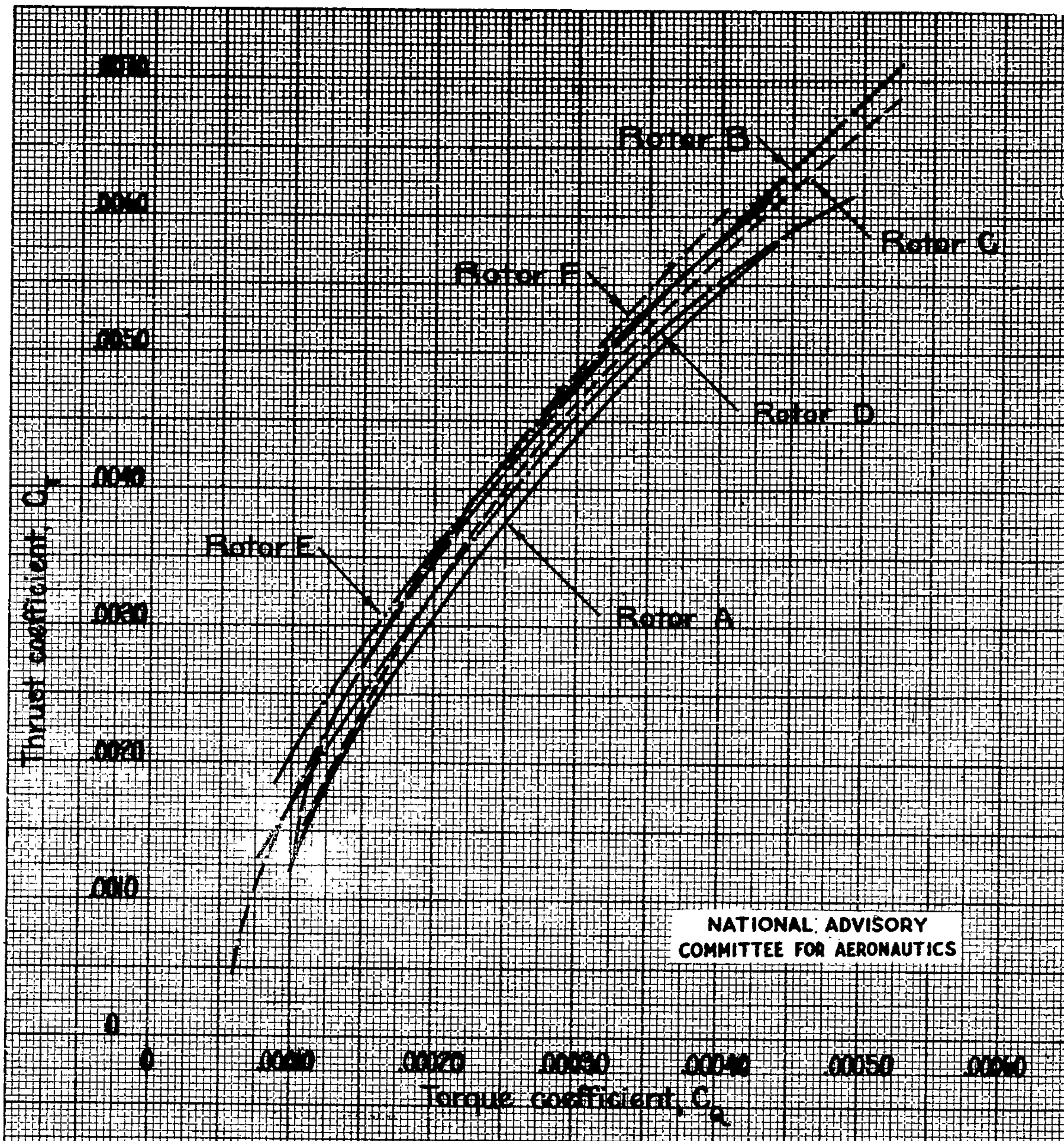

Figure 5.- Comparison of the static-thrust performance of the six rotors tested. (All coefficients are based on a 19-foot rotor-blade radius.)